Laser Innovations for Research and Applications
journal homepage: https://lira.journals.ekb.eg/
ISSN: Print 3009-6359 / Online 3009-6472

Exploring High–Order Distortions Associated with Directly Modulated Laser Diodes in Analog Optical Fiber Systems: The Role of Modulation Depth and Fiber Length

Moustafa Ahmed[1], Ghodran Abdullah[1], and Alaa Mahmoud[2*]

[1]Department of Physics, Faculty of Science, King Abdulaziz University, Jeddah, 80203 Saudi Arabia

[2]Laser Institute for Research and Applications, Beni-Suef University, Beni-Suef, 62511 Egypt

Abstract
This study investigates the impact of modulation depth and fiber length on high-order distortions in analog optical fiber systems employing directly modulated laser diodes with two-tone. High-order distortions, including 2nd– and 3rd–order harmonic distortions (HDs) and 3rd–order intermodulation distortions (IMD3), are modeled and analyzed in both time and frequency domains. The numerical simulation relies on the rate equations of laser diodes driven by an injection current containing two sinusoidal waves, spaced by a low radio frequency of 10 MHz. The results reveal the interplay between modulation depth and fiber length in minimizing distortions and identifying optimal operating ranges. The 2HD demonstrates the highest distortion level for modulation depth up to 0.4. Beyond this threshold, IMD3 becomes the predominant source of signal distortion. In contrast, 3HD exhibits the lowest distortion levels across the entire range of modulation depth. Fiber lengths shorter than 5 km minimize IMD3, while lengths around 5 km and 3 km minimize 2HD and 3HD, respectively These findings contribute to enhancing the performance of analog fiber communication systems, particularly in applications requiring high signal fidelity.

Keywords: Laser diodes, Direct modulation, Optical fiber systems, Distortions

*Corresponding author at: Laser Institute for Research and Applications LIRA, Beni-Suef University, Beni-Suef, Egypt

E-mail addresses: alaa.abutaleb@lira.bsu.edu.eg

1. Introduction

The growing demand for high-bandwidth communication has propelled the development and optimization of analog fiber systems, which are crucial for applications ranging from cable television distribution to radio over fiber technologies (Willner, 2019). The advancement of optical communication technology has considerably revolutionized the telecommunication industry, providing high-speed data transfer across great distances with minimum loss, which is an essential issue for many laser diode-based applications (Mahmoud et al., 2023).

Direct modulation of laser diodes is a typical method of converting electrical signals into optical signals. This approach provides numerous desirable properties in optical fiber communications, including compatibility with existing equipment, simplicity, cost-effective solutions, and the capability to modulate data at high frequencies (Ahmed et al., 2014; Agrawal, 2012). However, the photon and electron concentrations in the active medium are highly susceptible to nonlinear dynamic behaviors when the laser diode is modulated directly by RF signals (Lau & Yariv, 1984). These nonlinearities include leakage currents, gain suppression, and spatial hole burning, as well as relaxation oscillations (Odermatt et al., 2006; Morthier & Vankwikelberge, 2013). These nonlinear transfer properties introduce unwanted distortion products with the laser signals that were originally modulated. This degrades the signal quality and the system performance (Lau & Yariv, 1984). The common distortion products including higher-order harmonics that are generated at the multiples of the original frequencies, in addition to higher-order intermodulation distortions that are located very close to the original modulation frequencies (Jung & Han, 2002; Morton et al., 1989). Typically, the high-order distortions related to analog modulation of laser diodes with two-tone are harmonic distortions (HDs) and intermodulation distortions (IMD) (Morton et al., 1989; Mahmoud et al., 2016), which are increased around the laser relaxation oscillation (Bakry & Ahmed, 2013; Westbergh et al., 2008).

The critical challenge in analog fiber systems, such as radio over fiber (RoF) systems, cable television (CATV) networks, is the distortion introduced during signal transmission, which depends largely on the performance of direct modulation of laser diode (Yang, 2011). One significant factor influencing these distortions is the modulation depth of the laser diodes (Mahmoud et al., 2016; El-Salam et al., 2022; Bakry & Ahmed, 2016). Modulation depth determines the amplitude of the injected current, directly affecting the laser's output and consequently, signal distortions due to the effect of laser clipping (Qazi et al., 2014; Rainal, 1996). The laser clipping happens when the depth of modulation surpasses the threshold current of the laser, dropping the input current valleys under the threshold and hence, dropping the gain under the threshold level, resulting in almost nil output power and switching off the laser (Lai & Conradi, 1997). Another crucial factor that influences the distortion characteristics is the optical fiber. As the optical signal propagates down the fiber, it is subjected to various nonlinear properties, including attenuation and dispersion, which exacerbated with increasing fiber length, potentially increasing the distortions, adding further signal degradations (Ahmed et al., 2021; Mahmoud et al., 2022). This is attributed to the fact that the frequency chirp of the laser diode under direct modulation interacts with the optical fiber chromatic dispersion, resulting in distortions (Krehlik, 2006). Therefore, understanding the effects of laser modulation depth and fiber length on signal distortions is essential for optimizing the design and performance of analog fiber systems. Although previous studies in (Morton et al., 1989; Mahmoud et al., 2016; Bakry & Ahmed, 2013; El-Salam et al., 2022; Bakry & Ahmed, 2016; Qazi et al., 2014; Rainal, 1996; Ahmed et al., 2021; Mahmoud et al., 2022) have reported the influence of modulation laser parameters and fiber type on high-order distortions, the specific influence of modulation depth and fiber length on high-order distortions in analog fiber systems still needs to be adequately studied.

This paper introduces modeling and simulation of high-order distortions, including HDs and IMD3 that associated with laser diodes under two-tone direct modulation in analog fiber systems. The study focuses on how modulation depth and fiber length affect these high-order distortions. We employ a comprehensive modeling approach, investigating the modulated optical signal in both time and frequency domains in the free-running case as well as under the influence of fiber attenuation and dispersion. The model is based on the numerical integration of the rate equations governing laser diode operation, considering the injection of two sinusoidal waves spaced by a low frequency of 10 MHz. The main aim is to explore the optimal ranges of modulation depth and fiber length that minimize HDs and IMD3, thereby enhancing the performance of analog fiber communication systems.

2. Theoretical Model and Simulation Methodology

The dynamics of laser diode under direct modulation is analyzed using the model of laser rate equation, which describes the back-and-forth of energy between the number of photons *S* and number of injected carriers *N*. This laser rate model can be derived by the density-matrix method (Murray et al., 1974) or the traveling-wave method (Petermann, 2012). For a single-mode laser excited by DC, the rate equations are (Ahmed et al., 2007)

$$\frac{dN}{dt} = \frac{I}{eV} - \frac{N}{\tau_N} - G(N,S)S \tag{1}$$

$$\frac{dS}{dt} = \Gamma G(N,S)S - \frac{S}{\tau_p} + R_{sp} \tag{2}$$

where *e* is the charge of electron and *V* is the active medium volume, τ_N is the carrier lifetime due to spontaneous emission, τ_p is the photon lifetime which is the reciprocal of the total loss, is the mode confinement, and R_{sp} is the spontaneous emission factor. These rate equations can be solved numerically to show the laser dynamics in the transient regime, which influence the modulation characteristics of the laser. The optical gain *G* is described by the following form:

$$G = \frac{a\Gamma}{V}\frac{N - N_g}{1 + \varepsilon S} \tag{3}$$

where α is the linewidth enhancement factor, N_g is the electron number at transparency, and ε is the coefficient of nonlinear gain suppression. In the present case of semiconductor laser directly modulated by a time-harmonic current signal with two frequencies f_{m1} (modulation frequency of the first tone) and f_{m2} (modulation frequency of the second tone), the injection current $I(t)$ in equation (1) is given by the following form:

$$I(t) = I_b + I_m\left[\sin(2\pi f_{m1}t) + \sin(2\pi f_{m2}t)\right] \tag{4}$$

where I_b is the bias current and I_m is the modulation current, which define the modulation depth $m = I_m/I_b$. The second tone frequency f_{m2} is defined in terms of the frequency spacing Δf_m as $f_{m2} = f_{m1} + \Delta f_m$.

The optical power as a function of time $P(t)$ is calculated from the number of photons $S(t)$ via:

$$P(t) = \frac{\eta_o h\nu}{2\Gamma\tau_p} S(t) \tag{5}$$

where η_o is the differential quantum efficiency, ν is the optical frequency, and h is the Planck's constant.

The laser signal is sent down a standard single-mode fiber (SSMF) with dispersion D, attenuation coefficient α_f, and length L_f. The propagation of the laser signal down the optical fiber is described by equation:

$$\frac{\partial E}{\partial L} + \alpha_f E + iGVD(\omega_o)\frac{\partial^2 E}{\partial \tau^2} = 0 \tag{6}$$

where GVD refers to the group velocity dispersion, and ω_o is the reference frequency of the signal. The first term in equation (6) takes into account the slow change of the field (E) along the fiber length. The second term considers the fiber loss with α_f. The third term represents the first-order GVD, which accounts for the pulse broadening. GVD is converted into the wavelength domain parameters D (dispersion) via the relationship:

$$D = -\frac{2\pi c}{\lambda^2} GVD \tag{7}$$

The received power spectrum of the modulated signal $P(f)$ over time period T is calculated from the signal power $P(t)$ as (Ahmed et al., 2001)

$$P(f) = \frac{1}{T}\left|\int_0^T P(\tau) e^{-j2\pi f\tau} d\tau\right| \tag{8}$$

where f is the Fourier frequency.

The time trajectories of the laser power $P(t)$ are evaluated over sufficient long time expanding more than 256 cycles of period $T = 1/f_{m1}$. This calculation considers the longer half of the time trajectory of $S(t)$, which ensures that the laser transient characteristics are removed and the output remains stable. The power spectrum $P(f)$ in Eq. (6) is calculated by using the FFT of $P(t)$ as (Ahmed et al., 2001).

$$P(f) = \frac{\Delta t^2}{T} \left| FFT\left[P(t)\right] \right|^2 \tag{9}$$

The theoretical models described above are numerically solved using the professional Optisystem software. A schematic of the simulation software system design is shown in Figure 1. A carrier generator (CG) is used to generate two electrical signals at frequencies f_{m1} and f_{m2}. These two signals are used to modulate the laser diode (LD), which is injected simultaneously with bias current I_b and modulation current I_m. The modulation depth m is adjusted as $m = I_m/I_b$, with varying I_m while I_b remains constant. The optical power of the modulated laser signal is detected via the optical time-domain visualizer (OTDV), which displays the waveforms of the modulated laser signals. The modulated laser signal is then coupled to and propagates down a standard single-mode optical fiber (OF). Finally, a PIN photodiode (PD) detects the signals after passing fiber length L_f. The received electrical signals are displayed with the help of oscilloscope visualizer (OSC). The Fourier spectrum is measured via the RF spectrum analyzer (RFSA), which displays the frequency spectra of the modulated fundamental signals along with the high distortion products (harmonics and intermodulations). The calculations are applied to an InGaAsP DFB laser type emitting at wavelength of λ = 1.55 µm using the parametric values given in Table 1. The table is also includes the values of fiber link parameters.

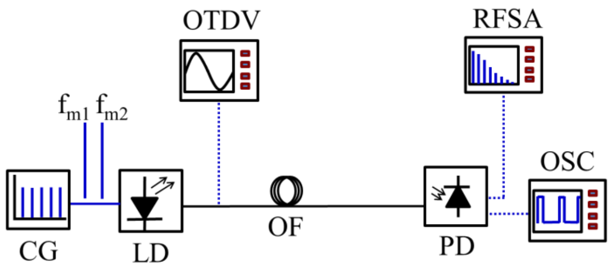

Fig. 1. Scheme of the designed system software for directly modulated laser diode with two-tone in analog optical fiber system.

Table 1. Typical values of DFB 1.55µm-InGaAsP laser, optical fiber and PIN photodiode parameters (Cartledge & Burley, 1989).

Parameter	Symbol	Value
Laser diode		
Wavelength	λ	1.55 µm
Active layer volume	V	1.5×10^{-16} m^3
Group velocity	v_g	8.5×10^9 cm/s
Quantum efficiency	η_o	0.4
Differential gain coefficient	a_o	2.5×10^{-20} m^2
Carrier density at transparency	N_g	1×10^{24} m^{-3}
Linewidth enhancement factor	α	5
Mode confinement	Γ	0.4
Carrier lifetime	τ_N	1×10^{-9} s
Photon lifetime	τ_p	3×10^{-12} s
Rate of spontaneous emission	R_{sp}	3×10^{-5}
Gain compression coefficient	ε	1×10^{-23} m^3
Optical fiber		
Attenuation coefficient	a_f	0.2 dB/km
Dispersion parameter	D	16.75 ps/nm/km
PIN photodiode		
Responsivity	R	1 A/W

3. Results and discussion

3.1 High–order distortions in the free-running laser operation case

The two–tone modulated laser signal waveforms of the free-running case (i.e., before coupled to and propagates down the fiber) with modulation depth of m = 0.01 (small signal), 0.2 (large signal) and 0.8 (deep signal) are shown in Figs. 2a, c, and e, respectively. The modulation frequency f_{m1} is set to the laser relaxation frequency f_r (= 5.25 GHz when the bias current I_b is twice the threshold current I_{th}) with frequency separation Δf_m = 10 MHz (i.e, f_{m2} = 5.26 GHz). In this instance, the high–order distortion products become more significant (Qazi et al., 2014). The insets of Figs. 2a, c, and e, display how the modulated laser signals deviate from the sinusoidal form of the modulating current $I(t)$ described in Eq. (4). Figure 2a demonstrates that the modulated laser signal is nearly sinusoidal at m = 0.01. When m increases to 0.2 and 0.8, the signals are clipped forming pulses as shown in insets of Figs. 2c and e, respectively. The clipping of the signals increases at the deep modulation of m = 0.8, which manifests as a character of distorted period doubling pulsation. This is attributed to the gain switching mechanism associated with the decrease of the lower cycles of the modulating current below the threshold current I_{th} at deep modulation (Ahmed & El-Lafi, 2008; Mahmoud & Ahmed 2021). These findings indicate high signal distortions as reported in (Bakry & Ahmed, 2016).

The corresponding Fourier frequency spectra displayed in Figs. 2b, d, and f, which reveal the evolution of distortion product powers with the increase of m. Figure 2d shows that at small signal modulation (m = 0.01), the powers of high–order distortion products are very weak. The spectrum displays only the fundamental peaks f_{m1} and f_{m2} along with the 2^{nd}–order harmonics ($2f_{m1}$ and $2f_{m2}$), as well as 2^{nd}–order intermodulation products ($f_{m1} + f_{m2}$). When m increases to 0.2 and 0.8, the powers of high–order distortion products are increase with the appearance of the 3^{rd}–order intermodulation products ($f_{m1} - \Delta f_m$ and $f_{m2} + \Delta f_m$) and 3^{rd}–order harmonics ($3f_{m1}$ and $3f_{m2}$), as well as insignificant weaker products as shown in Figs. 2d and f, respectively. Moreover, the spectrum in Fig. 2f indicates that at deep modulation (m = 0.8), the power of distortion products are significantly increase than that when m = 0.2 shown in Fig. 2d. The remarkable peaks at the high–order harmonics and 3^{rd}–order intermodulation products are particularly significant as they often exhibit the highest power level relative to other products (Bakry & Ahmed, 2016). The increase in 3^{rd}–order intermodulation products are probable lie within the transmission range of the fundamental tones f_{m1} and f_{m2}, and hence cannot be filtered out (El-Salam et al., 2022; Mahmoud et al., 2018), which manifests as an increase of 3^{rd}–order intermodulation distortion IMD3. In addition, the increase in 2^{nd}– and 3^{rd}–order harmonics manifests as the increase of the 2^{nd}– and 3^{rd}–order harmonic distortions, 2HD and 3HD, respectively. The distortion power levels recorded from these spectra are used to determine the IMD3, 2HD and 3HD using the following formulas (Bakry & Ahmed, 2016),

$$\mathrm{IMD3(dBc)} = 10\log_{10}\frac{P(f)_{f_{m1}-\Delta f}}{P(f)_{f_m}} \tag{10}$$

$$\mathrm{2HD\,(dBc)} = 10\log_{10}\frac{P(f)_{2f_m}}{P(f)_{f_m}} \tag{11}$$

$$\mathrm{3HD\,(dBc)} = 10\log_{10}\frac{P(f)_{3f_m}}{P(f)_{f_m}} \tag{12}$$

where $P(f)_{fm}$ is the power at the fundamental modulation frequency f_m, as well as $P(f)_{fm1} - \Delta f_{\mathrm{m}}$, $P(f)_{2fm}$ and $P(f)_{3fm}$ are the powers at 3rd–order intermodulation, 2nd–and 3rd–order harmonic products, respectively.

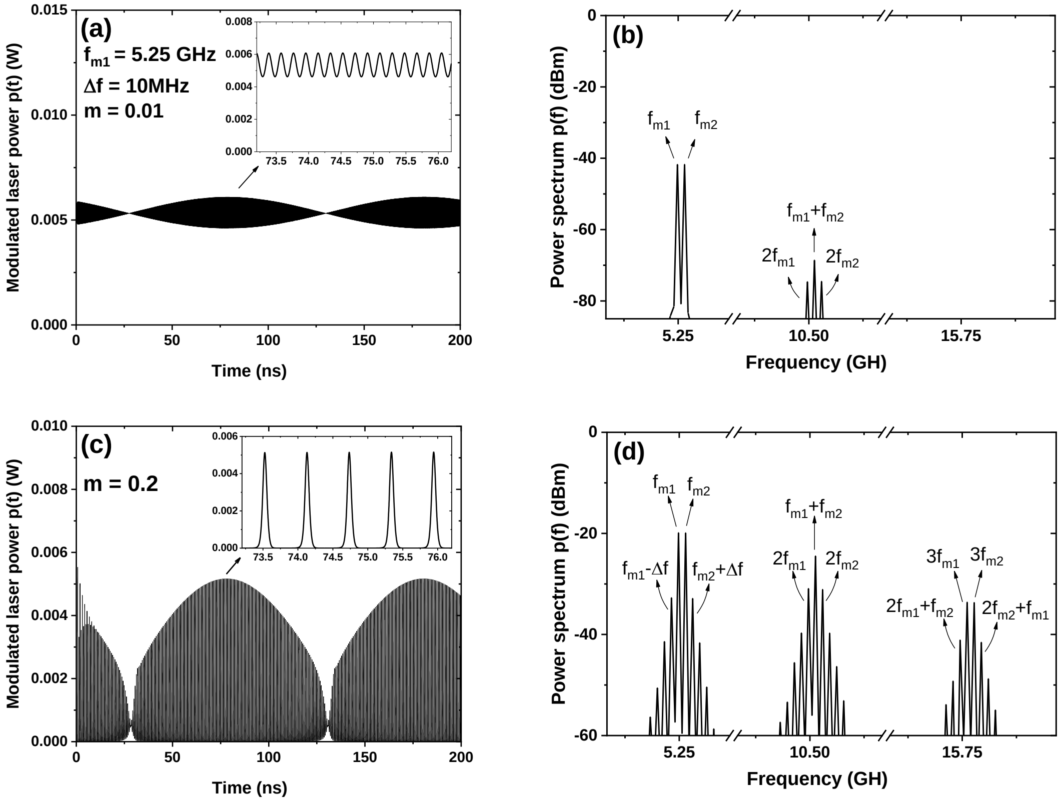

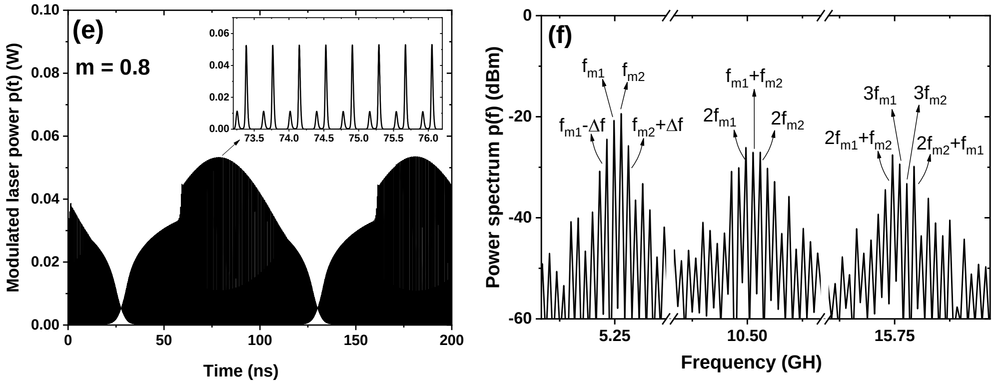

Fig. 2. (a), (c) and (e) The waveforms of the two-tone modulated laser signals, and (b), (d), and (f) Fourier frequency spectra of the received modulated laser signals and their high–order distortion products when f_{m1} = 5.25 GHz, Δf_m= 10 MHz and m = 0.01, 0.2 and 0.8, respectively.

The variations in modulated laser distortion types IMD3, 2HD, and 3HD during free-running laser operation over a wide range of modulation depth m are presented in Figs. 3a, b, and c, respectively. The data demonstrate that all types of distortion raises as the laser modulation depth increases. This behavior is consistent with the results reported in (Mahmoud et al., 2016) for two-tone modulation and (Mahmoud et al., 2018) for multi-tone modulation, both using the same laser parameters as this research. For modulation depth up to m = 0.4, 2HD exhibits the highest distortion level as illustrated in Fig. 3b. Beyond this point, IMD3 becomes the dominant source of signal distortion, as shown in Fig. 3a. In contrast, Fig. 3c shows that 3HD consistently remains the lowest distortion type across the entire range of m, which indicates an insignificant effect on the fundamental modulated laser signals.

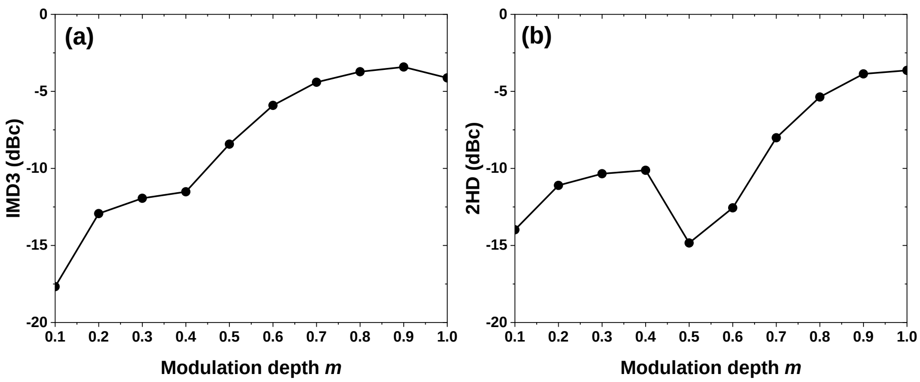

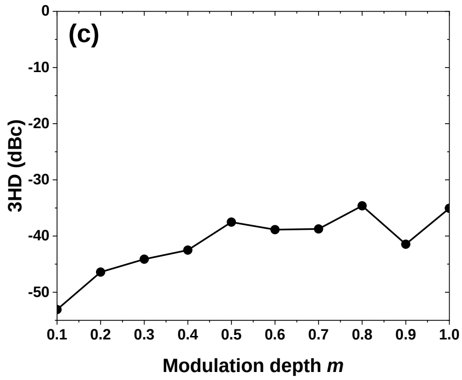

Fig. 3. Influence of the modulation depth m on the high–order distortion types of (a) IMD3 (b) 2HD and (c) 3HD when $I_b = 2I_{th}$ and $f_{m1} = 5.25$ GHz.

3.2 High–order distortions in the optical fiber system

The effect of the fiber length on the high–order distortions associated with the modulated laser signals are investigated with the limiting fiber properties; namely, attenuation and dispersion. To understand the intrinsic fiber attenuation influence on the distortion types, we ignore the fiber dispersion (i.e, $D = 0$) while the attenuation is enabled ($\alpha_f = 0.2$ dB/km) and vary the fiber length L_f. This implies that the third term in fiber propagation Eq. (6), which reflects GVD, is omitted, and the computations are thus limited to the first two terms. Figures 4a – c plot variation of the signal distortion types of IMD3, 2HD and 3HD, respectively when fiber length L_f ranges from 0 (without fiber, as the free-running case of laser operation) to 10 km at $m = 0.2$ and 0.8. The figures indicate that fiber attenuation has no significant effect on all distortion types, which is consistent with the results reported in (El-Salam et al., 2022). In contrast to the free-running laser operation case, the distortion levels are nearly constant as shown in Fig. 3 when $m = 0.2$ and 0.8.

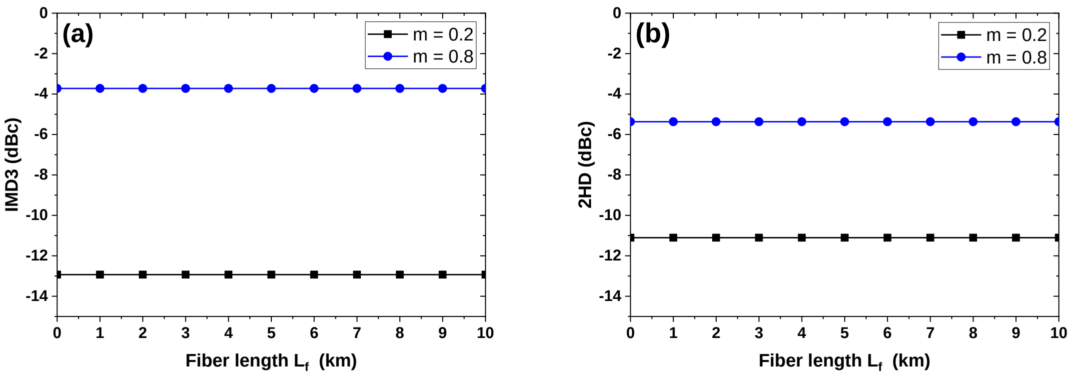

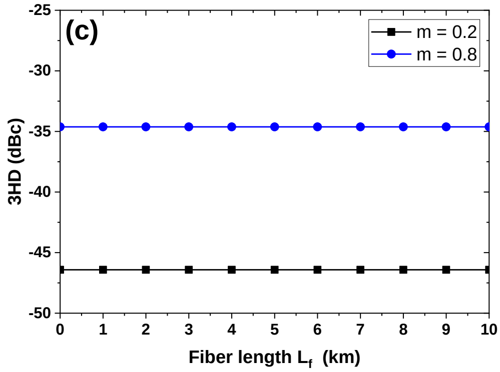

Fig. 4. Influence of fiber length L_f on distortion types of (a) IMD3 (b) 2HD and (c) 3HD when m = 0.2 and 0.8, considering the influence of attenuation only.

Figures 5a – d show the effect of fiber length L_f on the high–order distortion product powers associated with modulated laser signals when enabling the fiber dispersion (D = 16.75 ps/nm/km) at a modulation depth of m = 0.2. Comparing the frequency spectra reveals that IMD3, the critical distortion type (El-Salam et al., 2022; Mahmoud et al., 2018), increases as the L_f increase. For instance, the IMD3 increases from –12.89 to –12.79, –11.64 and –10.29 dBc when L_f increases from 1 to 3, 7 and 9 km, respectively. In contrast, the other distortion types (2HD and 3HD) exhibit varied behaviors that further investigation across an extended range of fiber lengths is necessary to fully understand their responses.

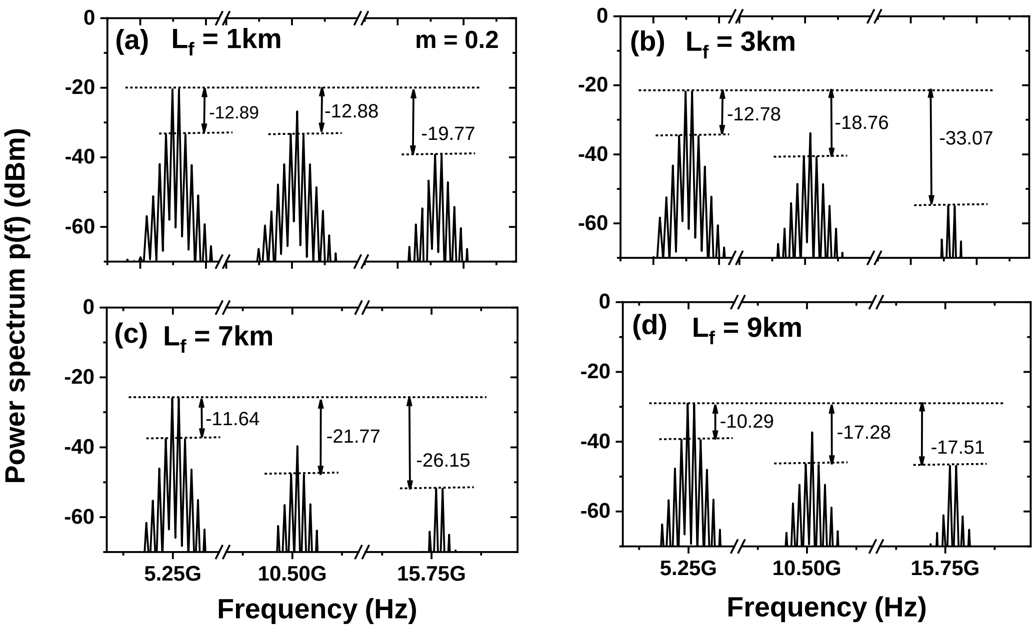

Fig. 5. Frequency spectra of the received modulated laser signals and their high–order distortion products when fiber dispersion is enabled at (a) L_f = 1km, (b) L_f = 3km, (c) L_f = 7km, and (d) L_f = 9km at m = 0.2.

Figures 6a – c show the effect of fiber length on the high–order distortions at m = 0.2 and 0.8. Fig. 6a shows that IMD3 raises with the increase of L_f, and the range of this increase gets wider with the increase of m; where the range is from –12.9 to –9.3 dBc when m = 0.2, whereas becomes from –3.7 to +7.4 dBc when m = 0.8. The figure shows also that when the fiber length L_f exceeds 5 km at m = 0.8, IMD3 happens to be larger than 0 dBc, which indicates that the intermodulation product exceeds the power level of the fundamental frequency fm1. Fig. 6b shows that 2HD exhibit similar behavior at the two modulation depths of 0.2 and 0.8 that they decrease with the increase of fiber length L_f, exhibits a minimum around L_f = 5 km, and then increases. Fig. 6c shows that 3HD exhibit almost similar behavior at the two modulation depths of 0.2 and 0.8 that they decrease with the increase of fiber length L_f, exhibits a minimum around L_f = 3 km, and then increases. We can conclude that transmitting the laser signal through an optical fiber with a length L_f shorter than 5 km can help minimize IMD3, while L_f ~ 5 and 3 km can help minimize 2HD and 3HD, respectively.

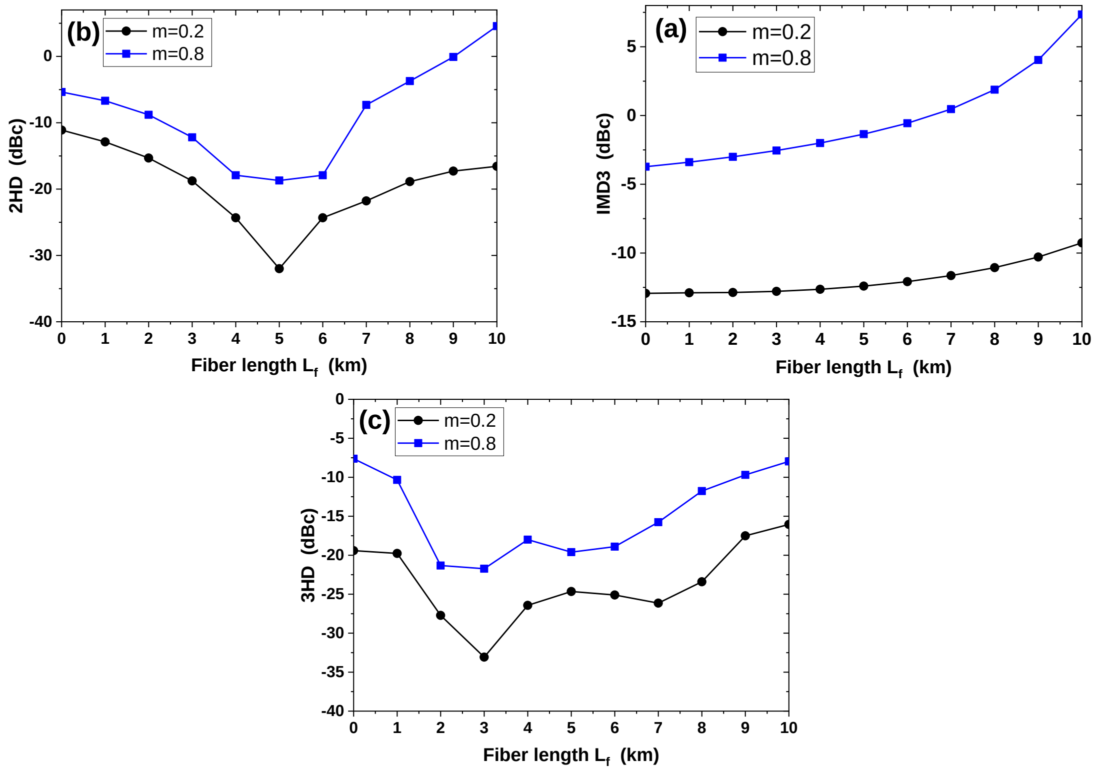

Fig. 6. Influence of fiber length L_f on distortions types of (a) IMD3 (b) 2HD and (c) 3HD when m = 0.2 and 0.8, considering the influence of dispersion.

4. Conclusion

This study comprehensively explores the role of modulation depth and fiber length in determining high-order distortions within analog optical fiber systems. The findings demonstrate that increasing modulation depth increases distortion levels, with 2nd–order harmonic distortion (2HD) dominating at moderate depths and 3rd–order intermodulation distortion (IMD3) becoming prominent at higher depths. The 3HD exhibits the lowest distortion levels across the entire range of *m*. Fiber attenuation has negligible effects on distortion levels, whereas dispersion significantly influences IMD3, 2HD, and 3HD, with optimal fiber lengths identified for minimizing these distortions. Fiber lengths shorter than 5 km minimize IMD3, while lengths around 5 km and 3 km minimize 2HD and 3HD, respectively. These findings provide practical guidelines for optimizing directly modulated laser diode systems in high-performance optical communication applications.

Funding: This research received no external funding.

Data availability: No datasets were generated or analyzed during the current study.

Conflict of interest: the authors declare no conflict of interest.

References

Agrawal, G. P. (2012). Fiber-optic communication systems. John Wiley & Sons

Ahmed, M., & El-Lafi, A. (2008). Large-signal analysis of analog intensity modulation of semiconductor lasers. Optics & Laser Technology, 40(6), 809-819.

Ahmed, M., Al-Hadeethi, Y., & Alghamdi, G. (2021). Influence of fiber properties on harmonic and intermodulation distortions of semiconductor lasers. Journal of Engineering Research and Reports, 20(7), 56-67

Ahmed, M., Mahmoud, S. W., & Mahmoud, A. A. (2014). Comparative study on modulation dynamic characteristics of laser diodes using RZ and NRZ bit formats. International Journal of Numerical Modelling: Electronic Networks, Devices and Fields, 27(1), 138-152.

Ahmed, M., Yamada, M., & Mahmoud, S. W. (2007). Analysis of semiconductor laser dynamics under gigabit rate modulation. Journal of applied physics, 101(3).

Ahmed, M., Yamada, M., & Saito, M. (2001). Numerical modeling of intensity and phase noise in semiconductor lasers. IEEE journal of quantum electronics, 37(12), 1600-1610.

Bakry, A., & Ahmed, M. (2013). Influence of sinusoidal modulation on mode competition and signal distortion in multimode InGaAsP lasers. Optics & Laser Technology, 50, 134-140

Bakry, A., & Ahmed, M. (2016). Harmonic and intermodulation distortions and noise associated with two-tone modulation of high-speed semiconductor lasers. Physics of Wave Phenomena, 24, 64-72

Cartledge, J. C., & Burley, G. S. (1989). The effect of laser chirping on lightwave system performance. Journal of lightwave technology, 7(3), 568-573.

El-Salam, Y. A., Mohamed, T., & Mahmoud, A. (2022). Effects of two-tone intensity modulation on signal distortion and noise in a semiconductor laser for radio-over-fibre applications. Pramana, 96(3), 151

Jung, H. D., & Han, S. K. (2002). Nonlinear distortion suppression in directly modulated DFB-LD by dual-parallel modulation. IEEE Photonics Technology Letters, 14(7), 980-982

Krehlik, P. (2006). Characterization of semiconductor laser frequency chirp based on signal distortion in dispersive optical fiber. Opto-electronics review, 14, 119-124.

Lai, S., & Conradi, J. (1997). Theoretical and experimental analysis of clipping-induced impulsive noise in AM-VSB subcarrier multiplexed lightwave systems. Journal of lightwave technology, 15(1), 20-30

Lau, K. Y., & Yariv, A. J. A. P. L. (1984). Intermodulation distortion in a directly modulated semiconductor injection laser. Applied Physics Letters, 45(10), 1034-1036.

Mahmoud, A., & Ahmed, M. (2021). Generation of frequency comb and its dependence on gain suppression in directly modulated semiconductor laser. Applied Physics B, 127(8), 111.

Mahmoud, A., Abd El-Salam, Y., Ahmed, M., & Mohamed, T. (2022). Effect of fiber properties and dispersion management on distortions associated with two subcarriers modulation of laser diode in radio over fiber systems. The European Physical Journal D, 76(11), 229

Mahmoud, A., Ahmed, M., & Mahmoud, S. W. (2018). Optimum parameters controlling distortion and noise of semiconductor laser under analog multichannel modulation. Pramana, 90, 1-8.

Mahmoud, A., Fouad, N., Ahmed, M., & Mohamed, T. (2023). Effect of linewidth enhancement factor of laser diode and fiber dispersion management on high-speed optical fiber links performance and use in WDM systems. Optical and Quantum Electronics, 55(2), 158.

Mahmoud, S. W., Mahmoud, A., & Ahmed, M. (2016). Noise performance and nonlinear distortion of semiconductor laser under two-tone modulation for use in analog CATV systems. International Journal of Numerical Modelling: Electronic Networks, Devices and Fields, 29(2), 280-290

Morthier, G., & Vankwikelberge, P. (2013). Handbook of distributed feedback laser diodes. Artech House

Morton, P. A., Ormondroyd, R. F., Bowers, J. E., & Demokan, M. S. (1989). Large-signal harmonic and intermodulation distortions in widebandwidth GaInAsP semiconductor lasers. IEEE Journal of Quantum Electronics, 25(6), 1559-1567

Murray, I.S., Iii Sargent, Marlan O. Scully, Willis E., Jr. Lamb, Laser Physics. 1st Edition ed. 1974, New York: Addison-Wesley Publishing Company.

Odermatt, S., Witzigmann, B., & Schmithüsen, B. (2006). Harmonic balance analysis for semiconductor lasers under large-signal modulation. Optical and Quantum Electronics, 38, 1039-1044.

Petermann, K. (2012). Laser diode modulation and noise (Vol. 3). Springer Science & Business Media.

Qazi, G., Sharma, A. K., & Uddin, M. (2014). Investigation on inter-modulation products (IMPs) for IM-DD SCM optical links. Optik, 125(5), 1629-1633

Rainal, A. J. (1996). Limiting distortion of CATV lasers. Journal of lightwave technology, 14(3), 474-479.

Westbergh, P., Söderberg, E., Gustavsson, J. S., Larsson, A., Zhang, Z., Berggren, J., & Hammar, M. (2008). Noise, distortion and dynamic range of single mode 1.3 µm InGaAs vertical cavity surface emitting lasers for radio-over-fibre links. IET optoelectronics, 2(2), 88-95.

Willner, A. (2019). Optical fiber telecommunications (Vol. 11). Academic Press

Yang, H. (2011). Optical techniques for broadband in-building networks, El-Salam, Y. A., Mohamed, T., & Mahmoud, A. (2022). Effects of two-tone intensity modulation on signal distortion and noise in a semiconductor laser for radio-over-fibre applications. Pramana, 96(3), 151.